

Modelling and Simulation of the Hybrid System PV-Wind

Alpha Alhaji BANGURA ¹, Mustapha ERROUHA ², Hicham HIHI ¹, Zakaria CHALH ^{1,*}

¹Engineering, Systems and Applications Laboratory, ENSA, Sidi Mohamed Ben Abdellah University, Fez, Morocco

²Plasma and Conversion of Energy Laboratory, ENSEITH, University of Toulouse, France

Abstract In this paper, we focused on modeling and simulation of a hybrid solar-wind energy system, consisting of a photovoltaic cell and a wind turbine driven by a Permanent Magnet Synchronous Generator (PMSG). The proposed system gives details of the hybrid solar-wind system. In the PV subsystem, there will be a photovoltaic energy subsystem, MPPT controller, and a DC-DC boost converter. The wind turbine subsystem includes a wind turbine energy subsystem, PMSG, and MPPT controller. The MPPT controllers were designed to extract the maximum power regardless of the weather conditions and temperatures. The P and O algorithm is introduced in the MPPT used in the PV energy subsystem and on the control of the machine side converter (MSC). The proposed wind turbine energy subsystem is based on Direct Torque and Flux Control (DTFC). The simulated results are demonstrated to show that the hybrid solar-wind generating system can realize a maximum power point tracking control of wind and solar power to satisfy the energy demand over an extensive range under unpredictable atmospheric conditions. The system has been demonstrated by MATLAB/Simulink and tested for variable weather conditions and temperatures.

Keywords Wind energy generator, Photovoltaic energy generator, Permanent Magnet Synchronous Generator (PMSG), Maximum Power Point Tracking (MPPT), DC-DC Boost Converter

DOI: 10.19139/soic-2310-5070-1535

1. Introduction

Energy is the most important of all resources. We need energy for light, to cook, and to keep us warm. The energy demand is constantly increasing, partly due to an increase in consumer needs, increasing population, and economic development. In recent years, wind energy and solar energy are considered alternative products in the energy electric system. Robust energy service is essential for economic development, to lift people out of poverty, increase the quality of education, and health services to empower women and children [1]. However, the majority of people living in developing countries (most of them located in rural areas) do not have access to any of the modern services including electricity, clean cooking, water purification, air conditioning, telecommunications, entertainment, and refrigeration [2]. Consequently, renewable energy resources (for example wind and solar) based off-grid become the most convenient solution to electrifying these areas [3][4][5].

In this paper, a hybrid solar-wind system is proposed to ensure a more stable energy-generating system. The proposed system ensures clean, reliable, and cheap energy on an annual basis. The system can adapt to the unpredictability of weather conditions and temperatures with two energy sources that can complement each other [3][6]. In other terms, the complementary nature between solar energy and wind energy. For example, there is high solar irradiation and relatively low wind energy in the daytime, while there is high wind energy but little irradiation at night[7][8]. The research includes using variable weather conditions and temperatures which are simulated in

*Correspondence to: Alpha Alhaji Bangura (Email: banguraa10@gmail.com). Engineering, Systems and Applications Laboratory, ENSA, Sidi Mohamed Ben Abdellah University, Fez, Morocco.

the MATLAB/Simulink environment to evaluate the efficiency of the system. The rest of the work is organized as follows. Section 2 provides a detailed analysis of the proposed system and the required electronic components (including interconnections). Section 3 describes the implementation of the PV system and its pilot strategy. Section 4 describes the implementation of the wind turbine system and its pilot strategy. Simulation results of the simulation are discussed in Section 5. Section 6 discussed modeling a Permanent Magnet Synchronous Generator (PMSG). Section 7 presents the results of the simulated proposed hybrid system. Finally, conclusions and references.

2. Proposed system description

The proposed system is made up of a wind turbine energy subsystem with a permanent magnet synchronous generator, a machine side converter, a direct torque, and flux control system, a PV energy subsystem, and a DC-DC boost converter. The hybrid solar-wind system is shown in Figure 1.

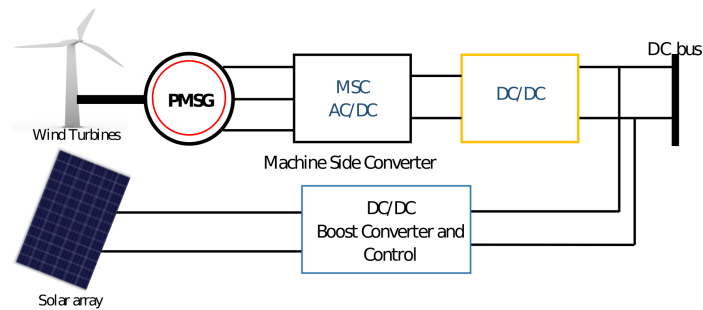


Figure 1. Diagram of the studied system.

3. Modelling of a Photovoltaic Generator

The PV cell (single diode) is modeled as a solar irradiance-dependent current source, photo-current (I_{ph}) in parallel with the diode [7]. The single diode model of PV cells is simple and easy to implement and show in the circuit diagram in Figure 1 below. The circuit model is represented in the following equations. The circuit consists of an ideal diode in parallel with a photo-current, generated by photons [7].

$$I_{rs} = I_{sc} / \left(\exp \frac{q \cdot V_d}{n \cdot K \cdot T} \right) - 1 \quad (1)$$

$$I_o = I_{rs} \left[\frac{T}{T_n} \right] \exp \left[\frac{q \cdot E_{go} \left(\frac{1}{T_n} - \frac{1}{T} \right)}{n \cdot K} \right] \quad (2)$$

$$I_{ph} = \frac{G}{G_{ref}} [I_{sc} + (K_i \cdot (T - T_n))] \quad (3)$$

$$I_{sh} = \frac{V + I R_s}{R_{sh}} \quad (4)$$

$$I = I_{ph} - I_o \cdot \left[\exp \frac{q(V + I \cdot R_s)}{n \cdot N_s \cdot K \cdot T} - 1 \right] - I_{sh} \quad (5)$$

$$I = I_{ph} - I_d - I_{sh} \tag{6}$$

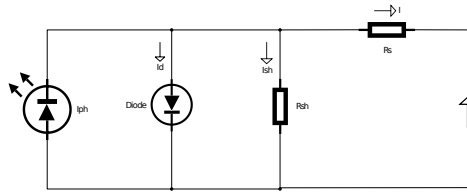


Figure 2. A single diode model of a PV cell circuit.

where I_{ph} is the photo generated current, I_d is the diode current, n is the ideality factor, I_o output current, K is Boltzmann constant, R_s is the series resistance, I_{sh} is the current across (R_{sh}) shunt resistance, V_d is the diode voltage, I_s saturation current of diode at T , and q is the charge on the electron.

3.1. Piloted strategy of the PV generator

Figure 3 shows a P and O pilot algorithm used in the PV energy subsystem. The MPPT calculates its location by oscillating on the power curve. From left to right, $\frac{dP}{dV} > 0$, the power increases while the voltage decreases[12]. From right to left, $\frac{dP}{dV} < 0$, the power decreases while the voltage increases[12]. At, $\frac{dP}{dV} = 0$ the photo-voltaic system reaches its maximum. The process has been simplified and shown in Figure 3.

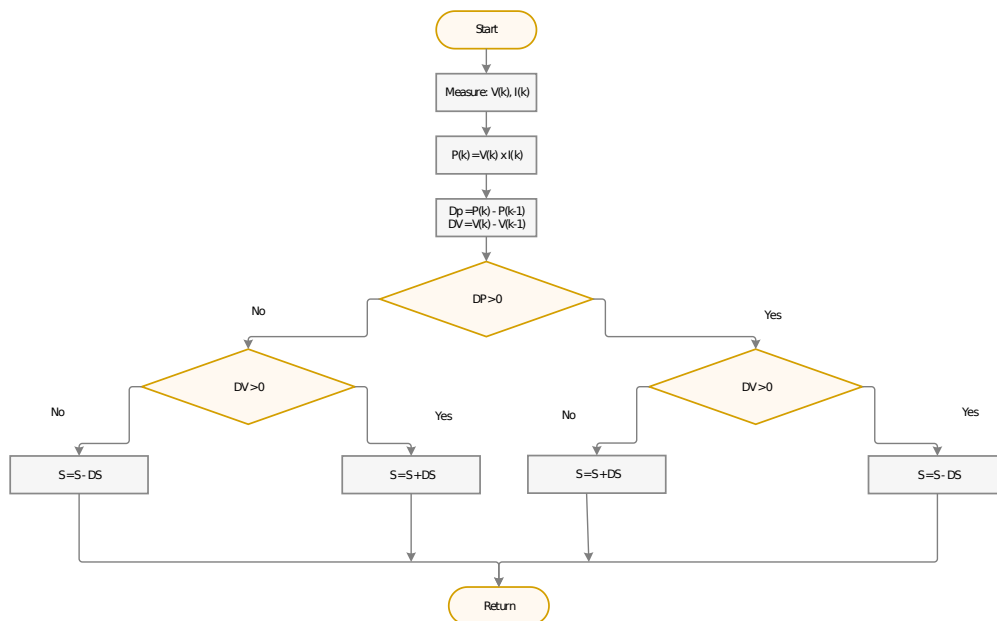


Figure 3. Diagram of pilot MPPT algorithm (P and O)

A change in light intensity on a photovoltaic cell affects the solar cell parameters, which include: short-circuit current I_{sc} , open-circuit voltage V_{oc} , and the efficiency of the cell. A reduction of sunlight resulting primarily in a reduction in current and consequently a reduced power output. At a constant temperature 25°C and variable irradianations, the characteristics of the $P(V)$ and $I(V)$ are shown in Figure 4[5].

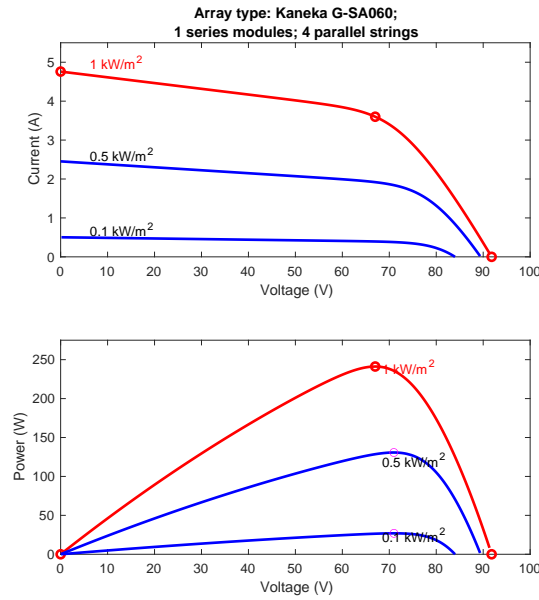


Figure 4. PV characteristics under variable weather conditions and constant temperature at 25°C

The output power and voltage of the DC-DC boost converter with a variation of radiation and temperature are shown in Figure 5[8].

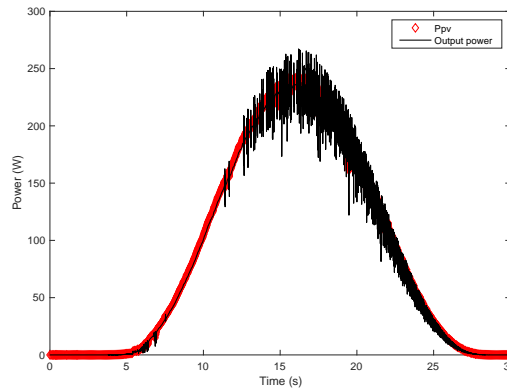


Figure 5. Photovoltaic generator characteristics when connected to DC-DC boost converter under variable irradianations I_{rrand} constant Temperature at 25°C

The variation curve of the DC signal at the DC-DC boost converter output obtained is shown in Figures 5 and 6. The output voltage of the PV cell is 67V, which is increased considerably with a variety of radiations while the current value at the output decreases[8].

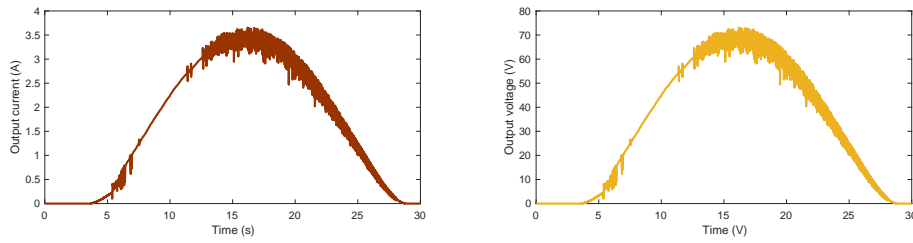


Figure 6. Voltage and current at the output of the boost converter.

Photovoltaic generator characteristics are shown in Table 1

Table 1. Kaneka G-SA060 module (60.3W) characteristics.

Parameters	Values
Ppm(W)	60.3
Vpm(V)	67
Ipm(A)	0.91
Rs(Ω)	0.161351
Isc(A)	1.19
Voc(V)	91.8
Ns	108
Rsh(Ω)	254.8275

The radiation is varied as shown in Figure 7: for the first few seconds, the irradiation is at its lowest, then it increases. Finally, it returned to its initial state when there was less penetration of the sun.

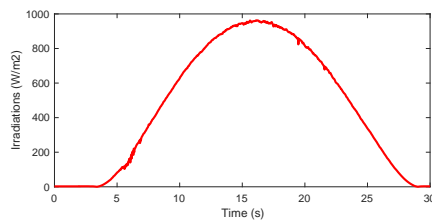


Figure 7. Variation of the radiation at 25°C

From Figure 8 below, we observed that a change in radiation leads to change in the output of the PV generator.

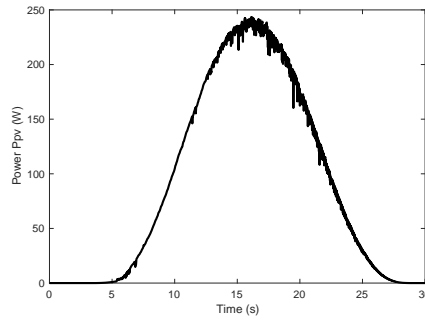


Figure 8. Output power of the photovoltaic generator.

4. Modulization of the wind turbine

The wind generator model comprises a wind turbine, a Machine Side Converter (MSC), a Direct Torque and Flux Control, and a PMSG that produces electricity from the mechanical energy obtained from the wind [8].

4.1. Modelling of the wind turbine

The wind turbine is a mechanical device that extracts the energy of moving air and converts it into useful work (Mechanical power that can be characterized by speed of rotation and mechanical torque)[9]. This work can be used for generating electrical power when combined with a generator[10]. The factors that determine the relationship between wind energy and the recovered mechanical energy are wind speed, air density, and the area swept by the rotor.

$$P_t = \frac{1}{2} C_p(\beta, \lambda) \rho \pi R^2 V_m^3 \quad (7)$$

The power coefficient varies depending on a given turbine[8][9]. The expression of the power coefficient has been approximated, for this turbine, the following C_p is given:

$$C_p = C_1 \left[\left(\frac{C_2}{\lambda \cdot i} \right) - C_3 \beta - C_4 \right] \exp \left(\frac{-C_5}{\lambda \cdot i} \right) + C_6 \cdot \lambda \quad (8)$$

And the tip speed ratio is demonstrated as:

$$\lambda = \frac{\Omega_m \cdot R}{V_m} \quad (9)$$

Where: C_1 to C_6 represents coefficients of wind turbine characteristics ($C_1=0.51$, $C_2=116$, $C_3=0.4$, $C_4=5$, $C_5=21$, and $C_6=0.0068$), β is the pitch angle, V_w is the wind speed, Ω_m is the turbine speed, ρ is the air density, R is the rotor radius, and λ is the tip speed ratio.

4.2. Piloted strategy of the wind generator

The Tip speed Ratio method is the technique that is commonly used to extract the maximum power because of its simplicity and independence to wind turbine characteristics. The algorithm consists of determining the speed of the wind which makes it possible to obtain the maximum power generated. This MPPT control strategy is without wind speed measurement. An optimal tip-speed ratio λ_{max} that corresponds to the maximum power coefficient (C_{pmax}) is fixed. Given the difficulties of measuring the wind speed, an estimate of its value can be obtained.

Control strategy for the Machine Side Converter (MSC):

The principle of Direct Torque and Flux Control is based on directly selecting the appropriate stator voltage vectors according to the differences between the reference and actual values of the magnitude of the stator flux vector and the electromagnetic torque[11]. In this research, the Direct Torque Control implementation is done with Space Vector Modulation (DTC-SVM). Space Vector Modulation is an algorithm for the control of Pulse Width Modulation (PWM)[11]. It ensures lower harmonics of stator current and allows to reduce the electromagnetic torque ripple. it also presents the possibility of maintaining the constant switching frequency[11].

5. Simulation Results

- Data and parameters of the wind turbine system; Rated power $P_{wt}=586W$ at 12.5m/s; diameter, $R=1.15m$.
- Data and parameters of PMSG generator: rated power $P_e=10kW$; stator resistance, $R_s=0.05\Omega$; stator dq-axis inductances, $L_d, L_q=0.645mH$; permanent magnet flux $\psi_f=0.192Wb$; rated speed, $n_s=100rad/s$; and pole pairs $P=4$.

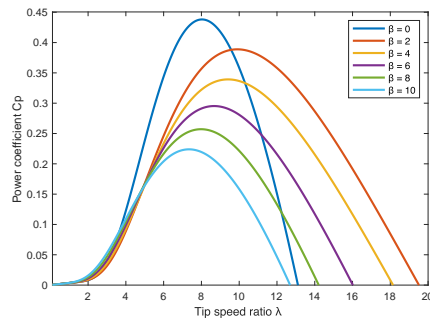


Figure 9. Curves of power coefficient C_p for different values of tip speed ratio λ and blade pitch angle β

Figure 9 shows that for each value of the blade pitch angle, there is a certain optimal value of the tip speed ratio for which the power coefficient reaches its maximum value. It also shows that the power coefficient is at its maximum $C_{pmax}=0.45$ at which $\lambda_{opt}=8.02$ and so do Figures 10 and 11 respectively.

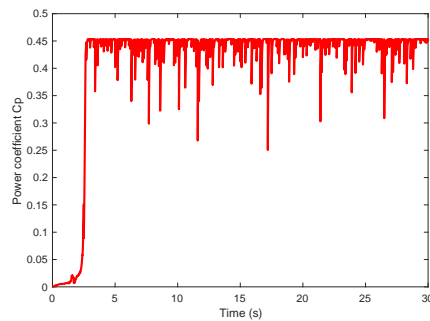
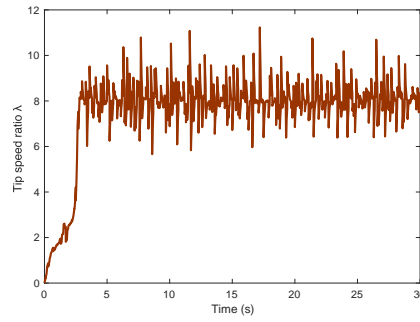


Figure 10. Power Coefficient C_{pmax}

Figure 11. Lambda optimal λ_{opt}

6. Modelling of the PMSG

PMSG is suitable for wind turbines as it is stable and secure during operation[11]. The PMSG choice allows direct-drive systems that avoid gearbox use thus low maintenance[10]. The mathematical model of the PMSG is divided into parts; electric, magnetic, and mechanical as defined by the following equations[11]:

Electric equations:

$$V_d = -R_s I_d - \frac{d\omega_d}{dt} + \omega_e \omega_q \quad (10)$$

$$V_q = -R_s I_q - \frac{d\omega_q}{dt} + \omega_e \omega_d \quad (11)$$

with

$$\omega_d = L_d L_q + \psi f \quad (12)$$

$$\omega_q = L_d L_q \quad (13)$$

$$\omega_e = P \omega_g \quad (14)$$

Electromagnetic torque:

$$T_{em} = \frac{1}{2} [(L_d - L_q) I_d I_q + I_q \psi f] \quad (15)$$

Mechanical equation:

$$T_m - T_{em} - f \Omega_m = J \frac{d\Omega}{dt} \quad (16)$$

Where: R_s is the stator resistance, (Ω) L_d and L_q are the inductances (H) of the generator on the d and q axes, ψ_f is the permanent magnetic flux (Wb), ω_e is the electrical rotating velocity of the generator (rad/s) of the PMSG rotor, T_{em} is the electromagnetic torque (N.m), T_m is the mechanical torque applied to the generator, f is the viscous coefficient of friction, J is the total moment of inertia of the machine, P is the number of generator pole pairs, ω_e and ω_g are respectively the electrical rotating velocity (rad/s) and the mechanical rotating velocity of the generator[13].

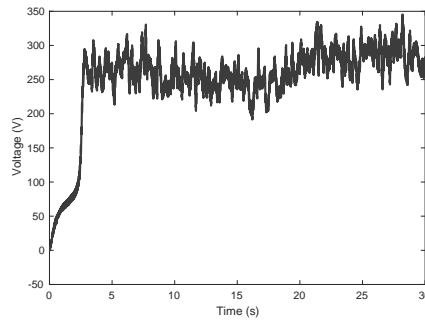


Figure 12. Output voltage Vdc of the wind turbine

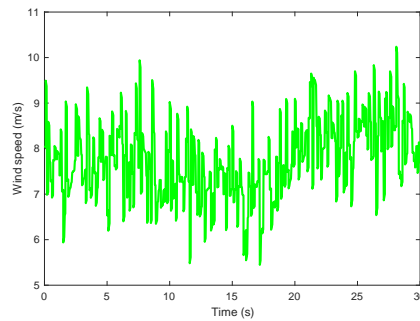


Figure 13. Variation of the wind speed.

In Figures 12 and 13, we observe that the output DC voltage and the output power follow the variation of the wind speed in Figure 14.

7. Hybrid system PV-Wind simulation

The hybrid system PV-Wind is made up of a Kaneka-GSA060; 1 series module; 4 parallel strings, Air X wind turbine driven by permanent magnet synchronous generator (PMSG). The power generated from the wind turbine, photovoltaic cell, and sum of wind/photovoltaic are shown in Figure 15 below. From the figure we observed that $P_{(pvw)}$ is the sum of the power generated from the wind turbine and photovoltaic cell.

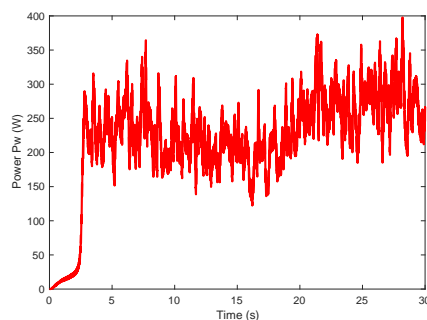


Figure 14. Wind turbine generator power.

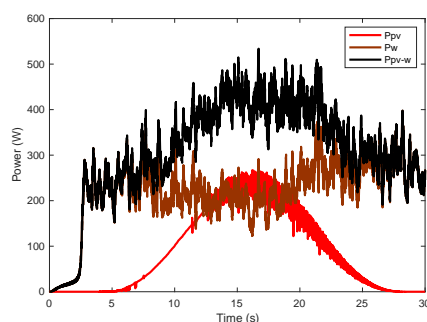


Figure 15. Photovoltaic, Wind, and sum of the wind and photovoltaic generators power

8. Conclusion

In this paper, modulization and simulation of a hybrid renewable energy system have been performed. The proposed system comprises a wind turbine energy subsystem with a permanent magnet synchronous generator and photovoltaic energy subsystem. The objective is accomplished by ensuring a stable desired power flow to the load under different weather conditions and temperatures. The simulation demonstrated the effectiveness of the proposed system. In summary, the proposed system and control strategy achieved their intended objectives.

REFERENCES

1. Phimister, Euan and Vera-Toscano, Esperanza and Roberts, Deborah, *The dynamics of energy poverty: evidence from Spain*, Economics of Energy & Environmental Policy, volume 4, pages 153–166, 2015, JSTOR.
2. Onyeji, Ijeoma and Bazilian, Morgan and Nussbaumer, Patrick, *Contextualizing electricity access in sub-Saharan Africa*, Energy for Sustainable Development, volume 16, pages 520–527, 2012, Elsevier.
3. Phimister, Euan and Vera-Toscano, Esperanza and Roberts, Deborah, *Global energy outlook 2019: the next generation of energy*, Resources for the Future, pages 8–19, 2019.
4. Carrasco, LM and Martín-Campo, F Javier and Narvarte, L and Ortuño, M Teresa and Vitoriano, Begoña, *Design of maintenance structures for rural electrification with solar home systems. The case of the Moroccan program*, Energy, volume 117, pages 47–57, 2016, Elsevier.
5. Khan, Jibran and Arsalan, Mudassar H, *Solar power technologies for sustainable electricity generation—A review*, Renewable and Sustainable Energy Reviews, volume 55, pages 414–425, 2016, Elsevier.
6. Micangeli, Andrea and Fioriti, Davide and Cherubini, Paolo and Duenas-Martinez, Pablo, *Optimal Design of Isolated Mini-Grids with Deterministic Methods: Matching Predictive Operating Strategies with Low Computational Requirements*, Energies, volume 13, pages 16–4214, 2020, Multidisciplinary Digital Publishing Institute.
7. Allani, Mohamed Yassine and Jomaa, Manel and Mezghani, Dhafer and Mami, Abdelkader, *Modelling and simulation of the hybrid system PV-wind with MATLAB/SIMULINK*, 2018 9th International Renewable Energy Congress (IREC), pages 1–6, 2018, organization=IEEE.

8. Bellia, Habbati and Youcef, Ramdani and Fatima, Moulay, Pablo, *A detailed modeling of photovoltaic module using MATLAB*, NRIAG Journal of Astronomy and Geophysics, volume 3, number 1, pages 53–61, 2014, Taylor & Francis.
9. Gam, Olfa and Abdelati, Riadh and Abdou Tankari, Mahamadou and Mimouni, Mohamed Faouzi, *An improved energy management and control strategy for wind water pumping system*, Transactions of the Institute of Measurement and Control, volume 41, number 14, pages 3921–3935, 2019, SAGE Publications Sage UK: London, England.
10. Mayouf, Messaoud, *Contribution à la modélisation de l'aérogénérateur synchrone a aimants permanents*, 2018, Batna, Université El Hadj Lakhdar. Faculté des sciences de l'ingénieur.
11. Zelechowski, Marcin *Space vector modulated–direct torque controlled (dte–svm) inverter–fed induction motor drive*, Praca doktorska, Politechnika Warszawska, Wydział Elektryczny, Warszawa, 2005.
12. Micangeli, Andrea and Fioriti, Davide and Cherubini, Paolo and Duenas-Martinez, Pablo, *Singh, Bharat and Singh, SN*, Electric Power Components and Systems, volume 37, pages 427–440, 2009, Taylor & Francis.
13. Tahiri, Fatima Ezzahra and Chikh, Khalid and Khafallah, Mohamed, *Designing a Fuzzy-PI Controller of a Stand-Alone Wind Energy Conversion System for MPPT*, The Proceedings of the Third International Conference on Smart City Applications, volume 13, pages 1093–1106, organization=Springer, 2018.